Proposed for presentation at the Microcirculatory Society 54th Annual Meeting, Washington DC, April 28-May 2, 2007

Microvascular Branching as a Determinant of Blood Flow by Intravital Particle Imaging Velocimetry

Patricia Parsons-Wingerter, Terri McKay, Mary Vickerman,
Mark P. Wernet, Jerry G. Myers, Jr., Krishnan Radhakrishnan

The effects of microvascular branching on blood flow were investigated in vivo by microscopic particle imaging velocimetry (micro-PIV). We use micro-PIV to measure blood flow by tracking red blood cells (RBC) as the moving particles. Velocity flow fields, including flow pulsatility, were analyzed for the first four branching orders of capillaries, postcapillary venules and small veins of the microvascular network within the developing avian yolksac at embryonic day 5 (E5). Increasing volumetric flowrates were obtained from parabolic laminar flow profiles as a function of increasing vessel diameter and branching order. Maximum flow velocities increased approximately twenty-fold as the function of increasing vessel diameter and branching order compared to flow velocities of 100 – 150 micron/sec in the capillaries. Results from our study will be useful for the increased understanding of blood flow within anastomotic, heterogeneous microvascular networks.

National Aeronautics and Space Administration

Microvascular Branching as a Determinant of Blood Flow by Intravital Particle Imaging Velocimetry

Experimental Biology
Microcirculatory Society
Vascular Biology Session
484.10:C46

Patricia Parsons-Wingerter,[1] Terri L. McKay,[1] Mary B. Vickerman,[1] Mark P. Wernet,[1]
Jerry G. Myers, Jr.,[1] and Krishnan Radhakrishnan[2]

[1]NASA Glenn Research Center, Cleveland, OH 44135, [2]University of New Mexico, School of Medicine, Department of Pathology and The Cancer Research & Treatment Center, Albuquerque, NM 87131

ABSTRACT

The effects of microvascular branching on blood flow were investigated in vivo by microscopic particle imaging velocimetry (micro-PIV). We use micro-PIV to measure blood flow by tracking red blood cells (RBC) as the moving particles. Velocity flow fields, including flow pulsatility, were analyzed for the first four branching orders of capillaries, postcapillary venules and small veins of the microvascular network within the developing avian yolksac at embryonic day 5 (E5). Increasing volumetric flowrates were obtained from the flow profiles as a function of increasing vessel diameter and branching order. Maximum flow velocities increased approximately twenty-fold with increasing vessel diameter and branching order relative to flow velocities of 100 – 150 μm/sec in the capillaries. Results from our study will be useful for advancing the understanding of blood flow within anastomotic, heterogeneous microvascular networks. (Supported by NASA Glenn Research Center IRD04-54.)

INTRODUCTION

It is hypothesized that the dynamics of blood flow, including velocity, pressure and shear stress, are influential factors in microvascular remodeling and angiogenesis. Blood flow is primarily laminar and therefore by Hagen-Poiseuille's law, blood flow and pressure are proportional to the fourth power of vessel radius (r^4). Our research focuses on the role of vessel morphology in microvascular remodeling, angiogenesis and lymphangiogenesis. We quantify vascular remodeling as a function of vessel morphology, diameter, branchpoint and branching generation using the NASA Glenn computer software VESGEN.[1-4] For this study, we are investigating blood flow as a function of vessel diameter by intravital particle imaging velocimetry (PIV).[5] PIV measures local velocities within a flow field by frame-to-frame cross-correlation of particle displacement. We image the optically accessible microvasculature of the avian embryonic yolk sac. Red blood cells (RBC) serve as the moving particles, so that fluorescent tracking particles are not required.

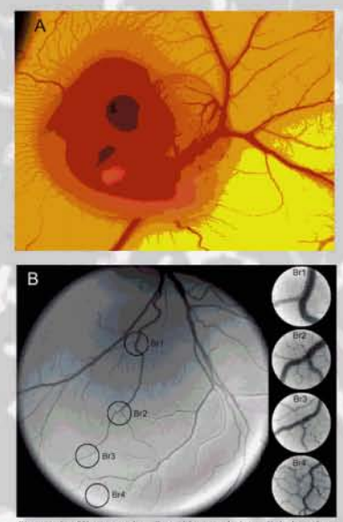

Figure 1. Microvascular Branching and Intravital Imaging. (A) Fertilized quail eggs were cultured ex ovo in 6-well Petri dishes until embryonic day 5 (E5). The yolksac vasculature, which transports blood pumped by the embryonic heart, is clearly visible on the yolk. (The chorioallantoic membrane (CAM) appears as a small, highly vascularized balloon exiting from the embryonic gut). **(B)** A representative venous vascular tree of the yolk sac containing four areas selected for imaging of Br1-Br4 is displayed.

METHODS

Intravital Imaging and Post-Processing. Fertilized quail eggs (*Coturnix coturnix japonica*) were cultured within 6-well Petri dishes at 37.5°C as described previously.[1-4] At embryonic day 5 (E5), a field of venous blood vessels was selected from the yolk sac vasculature (Fig. 1A) for the imaging of four successive vessel branchpoints (Br1-Br4) that included successive venous branching generations and capillary vessels (Fig. 1B). The Petri dish was placed on a microscope stage pre-warmed to 37°C and also under an infrared heat lamp. A digital image stack (or movie, Fig. 2A) of 375 images (image size of 1024 x 1024 pixels at 125 frames per sec and 1/300 sec shutter speed) was acquired in grayscale (256 levels) at total magnification of 144X (resolution = 0.957 μm/pixel) with an Olympus SZX12 stereo microscope and a high-speed, high-resolution Photron Ultima APX-RS CMOS sensor camera and Photron FastCam Viewer (PFV) software, illuminated by a 100W mercury burner light source with UV filter. A set of four image stacks, Br1-Br4, was acquired from each of five embryonic specimens; one representative image set is reported here. Images were despeckled by subtracting from each image a spot image obtained by processing the image stack with stack averaging, background subtraction, and histogram adjustment. Noise was reduced by slight Gaussian filtering. A binary vascular mask displaying only the vascular field was generated by reading the aligned images as an ImageJ stack, calculating the standard deviation image, and performing limited additional noise removal and thresholding (Fig. 2B). Images were aligned using the inverse of the vascular mask with NIH ImageJ plug-in TurboReg. The vascular mask also served to isolate the vascular velocity field for analysis by PIV.

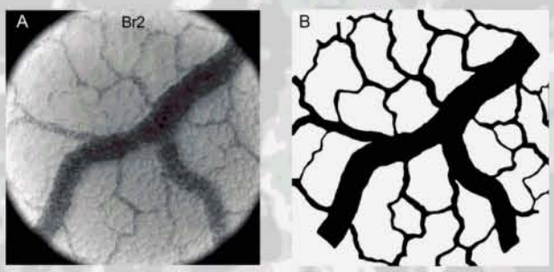

Figure 2. Imaging and Masking of a Vascular Field. (A) A gray-scale image from the Br2 image stack illustrates vascular morphology and blood flow. **(B)** The binary vascular mask of the Br2 image stack was used to (1) align the image stack and (2) isolate the vasculature for analysis of blood flow velocity by PIV.

Microscopic Particle Imaging Velocimetry (Micro-PIV). Microscopic PIV (micro-PIV) was performed on Br1-Br4 image sets using the NASA PIVPROC software program[5] to measure local velocities at each point on the image grid generated by a subregion size of 64x64 pixels and spacing of 32x32 pixels (for second pass: 32x32 pixels and 16x16 pixels, respectively). Background velocities (i.e., velocities in tissue outside of the blood vessels) within an image stack were set to zero using the vascular mask (Fig. 2B). PIVPROC employs advanced cross-correlation and particle tracking operations following background subtraction, and uses fuzzy logic for validating the identification of correlation peaks and particle pairings in particle-tracking operations.

Analysis of Blood Flow Velocity and Volumetric Flowrate. To resolve flow pulsatilities resulting from periodic velocity cycles due to cardiac pumping of the blood, the velocity field generated by PIVPROC for each image within a 375-image stack of Br1-Br4 was averaged over seven time steps (i.e., three images before, and three images after, the analyte image). The velocity field of blood flow in an image was converted by the scientific visualization software Ensight to a colorized map of velocity vectors. Average velocities were further calculated for the rise, peak, fall and valley of the periodic velocity cycle. The volumetric flowrate was calculated at each cross-section of a vessel by numerically integrating the velocity profile.

RESULTS

Results for a Br1-Br4 image set from a representative experiment with one specimen are illustrated in Figs. 3-4. Cross-sectional velocity profiles in the post-capillary collecting veins were approximately parabolic, indicating laminar blood flow. According to mean values of the cross-sectional cuts (red, green and blue, Fig. 3), the volumetric flowrate of 1.32 μl/min at maximum (peak) velocity in the largest vessel of Br1 (diameter = 169 μm) decreased to 1.17 μl/min at minimum (valley) velocity. The volumetric flowrate at maximum velocity in the largest vessel of Br4 (diameter = 74 μm) was 6.02×10^{-2} μl/min. Overall, the maximum flow velocity at the center of the vessels for Br1-Br4 decreased approximately 20X, from a maximum of 2000 μm/sec for the largest vessel in Br1 to 100-150 μm/sec in smaller capillaries (for example, see Br4). Absolute differences in the spatial average of velocity over time declined considerably from Br1 to Br4. Pulsatile flow cycles in Br1 – Br4 were approximately equal (0.4 sec).

DISCUSSION

By intravital micro-PIV, velocity flow fields were investigated for the first four branching orders of the microvascular network in the quail yolksac at E5. Blood flow was measured by tracking RBCs as the moving particles. Parabolic velocity profiles in the larger veins indicate that blood flow was laminar. By measurements of individual venous vessels, blood velocity and volumetric flowrate decreased with decreasing vessel size (Fig. 3), which is qualitatively consistent with the Hagen-Poiseuille law. In future calculations, we will investigate the mathematical relationship between vessel diameter, velocity and volumetric flowrate in our experimental model. By spatial averaging of the velocity flow field (Fig. 3), absolute differences in maximum and minimum averaged velocities for periodic flow cycles also decreased with decreasing branching order (Fig. 4). We will conclude our study by segmenting capillaries and veins in the velocity flow fields of Br1 – Br4 using the GRC software VESGEN (Fig. 5).[1-4] Segmentation (classification) of the vessels into generational branching orders will support further morphological analysis of blood flow dynamics as determined by vessel parameters that include vessel diameter, branchpoint density, and tortuosity.

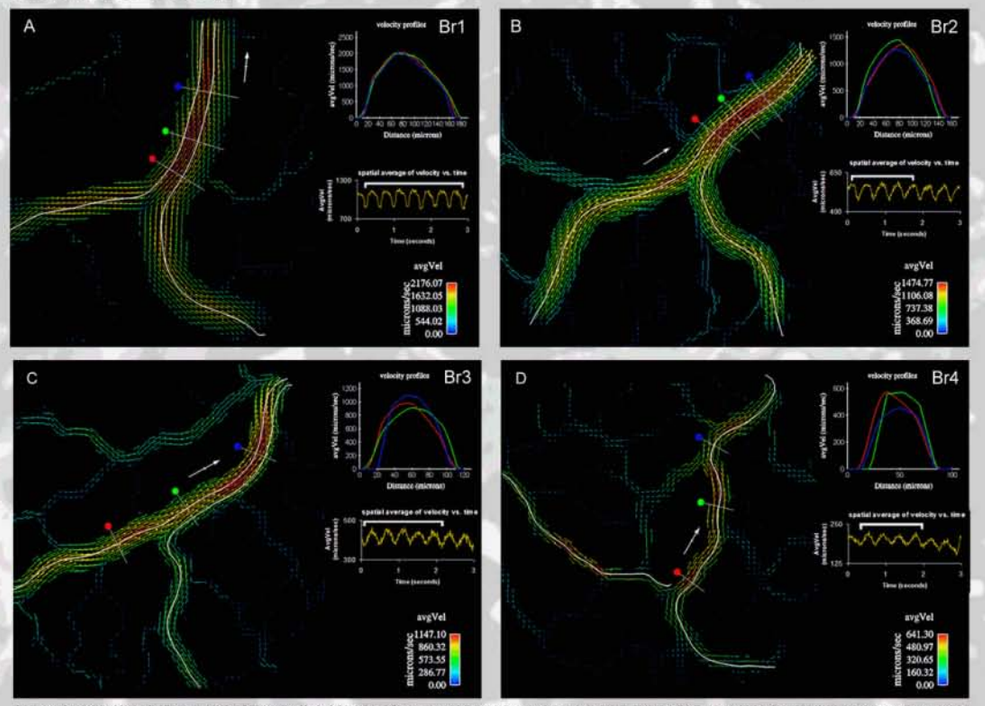

Figure 3. Analysis of Velocity Flow Fields for Successive Vessel Branching Generations. Velocity flow fields measured by micro-PIV and averaged for values of peak flow are illustrated for Br1-Br4 **(A-D)**, where the magnitude of the velocity vectors (μm/sec) are given by color lookup tables (LUT). Velocity profiles across the major vessels show good agreement, as generated by cross-sectional cuts (red, green, and blue circles), and are plotted in the upper right corner of the figure panels. The white arrows indicate the direction of venous flow, and the white lines are calculated particle path lines for the RBCs. Average velocities decreased considerably with decreasing vessel diameter. Velocity profiles are highly parabolic, indicating that blood flow within the vessels was laminar. Cyclic pulsatilities of the venous blood flow circulation are displayed in graphs of average velocity versus time (gold, center right).

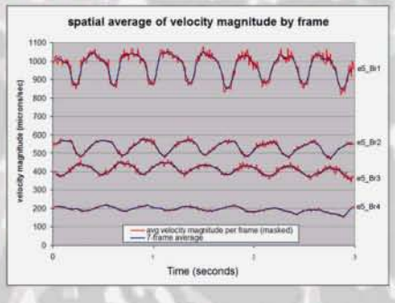

Figure 4. Comparison of Pulsatile Flow Magnitude and Cycle for Br1-Br4. The spatial average of the velocity flow field within each masked image of the 375 image stack is plotted versus time in red (frame-by-frame) and blue (7-frame average). The averaged velocity magnitude increased up to fivefold in the flow field containing the largest vessels (Br1), relative to the flow field of smallest vessels (Br4). Absolute differences in the average velocity of peak-to-valley blood flow decreased considerably from Br1 to Br4. The periodic cycles of pulsatile flow for Br1-Br4, however, were approximately equal (0.4 sec).

Figure 5. VESGEN Software for Automatic Analysis of Vessel Branching Generations (G1-G5). The VESGEN software analyzes numerous vessel parameters such as vessel diameter, length, tortuosity and number density for each generation of branching within a vascular tree (soon to be released by NASA Glenn as a downloadable software plug-in for NIH ImageJ).[1-4] As a final study for our project, velocity flow fields Br1-Br4 measured by micro-PIV will be analyzed according to vessel branching generation as determined by VESGEN.

1. Parsons-Wingerter P, Chandrasekharan UM, McKay TL, Radhakrishnan K, DiCorleto PE, Albarran B, Farr AG, The $VEGF_{165}$-Induced Phenotypic Switch from Increased Vessel Density to Increased Vessel Diameter and Increased Endothelial NOS Activity, *Microvasc Res* 2006, 72(3):91-100
2. Parsons-Wingerter P, McKay TL, Leontiev D, Vickerman MB, Condrich TK, DiCorleto PE: Lymphangiogenesis by blind-ended vessel sprouting is concurrent with hemangiogenesis by vascular splitting, *Anat Rec A Discov Mol Cell Evol Biol* 2006, 288:233-247
3. Parsons-Wingerter P, Elliott KE, Farr AG, Radhakrishnan K, Clark JI, Sage EH: Generational analysis reveals that TGF-beta1 inhibits the rate of angiogenesis in vivo by selective decrease in the number of new vessels, *Microvasc Res* 2000, 59:221-232
4. Parsons-Wingerter P, Elliott KE, Clark JI, Farr AG: Fibroblast growth factor-2 selectively stimulates angiogenesis of small vessels in arterial tree, *Arterioscler Thromb Vasc Biol* 2000, 20:1250-1256
5. Wernet MP, Digital Particle Image Velocimetry, Chapter in *Optical Metrology for Fluids, Combustion and Solids*, CR Mercer, Editor, Kluwer Academic Publishers, Boston 2003

Patricia Parsons-Wingerter, Ph.D.
NASA Glenn Research Center
21000 Brookpark Rd MS 110–3
Cleveland, OH 44135
Tel. 1–216–433–8796, Fax 1–216–433–3793
E-mail: patricia.parsons@grc.nasa.gov

www.nasa.gov

P–1070 Apr 07